J Mater Sci (2010) 45:2165–2173
DOI 10.1007/s10853-009-4055-x

HTC2009

Solidification behaviour of ceramic particle reinforced Al-alloy matrices

A. E. Karantzalis · A. Lekatou · E. Georgatis · H. Mavros

Received: 14 June 2009 / Accepted: 21 November 2009 / Published online: 9 December 2009

Abstract Novel metal matrix composites have been produced by cast production route. TiC and WC ceramic reinforcing particles have been successfully introduced into Al 6060, Al 319, Al 356, Al–7Si–5Mg, Al–20Cu and Al 2007 alloys. Refined grain structure and various intermetallic phase formation have been observed. Particle–melt and particle–solidification front interactions, solidification sequence and particle–matrix interfacial characteristics have been examined by means of metallography, SEM examination and EDX analysis. Particle distribution, intermetallic phase formation and location and grain structure are discussed in terms of ceramic-melt wetting characteristics, alloying element interfacial segregation and particle–solidification front thermal behaviour.

Introduction

During the last four decades, Particulate Reinforced Aluminium Matrix Composites (PRAMCs) have gained great research attention as attractive materials for potential industrial applications. This interest stems from property improvements, regarding strength and stiffness, density, high temperature properties, abrasion and wear resistance and damping capacities [1].

Quite a few different manufacturing and processing routes have been explored and proposed, based on either solid or liquid matrix state. The stir casting process is one of the most important ones, mainly due to cost and ease-to-handle considerations. Extensive research effort has been conducted, in order to investigate and understand the various phenomena governing the particle–matrix interactions during and after the solidification process. A thorough, in depth review for these phenomena can be found in the work of Rohatgi et al. [2]. However, it is considered necessary to address the main aspects concerning the final microstructure of a stir-cast metal matrix composite [1–6].

Two fundamental phenomena are responsible for the particle distribution and the final microstructure, and, consequently, the composite properties and performance. These are the particle–liquid metal interactions and the particle–solidification front interactions.

Regarding the particle–molten metal interactions, the particle–melt compatibility influences the initial particle distribution within the liquid melt. The particle–melt compatibility is assessed by means of wettability, i.e. the tendency of the liquid melt to spread over the surface of a ceramic substrate forming a low ($<90^{o}$) contact angle during the well-known sessile drop experiment [3, 5, 6]. Especially in the case of cast metal composites, however, a contact angle of less than 90 °C is not sufficient enough to lead to spontaneous entry of the particles but a 0 °C contact angle (total spreading condition) is required as shown by the works of Nakae et al. [7], Wu et al. [8] and Kaptay [9–11]. The involved surfaces may be poisoned by oxide phases or absorbed gases. Especially in the case of Al alloys, the presence of oxides and/or absorbed gases can significantly change their wetting characteristics, whereas their absence can make the wetting behaviour very favourable [12, 13].

Regarding the particle–solidification front interactions, these influence the final particle distribution and location. The particles can be pushed by the solidification front, engulfed by the solidification front or act as solid phase nucleation sites. Many theories have been developed

A. E. Karantzalis (✉) · A. Lekatou · E. Georgatis · H. Mavros
Department of Materials Science and Engineering,
University of Ioannina, 45110 Ioannina, Greece
e-mail: alexkarantzalis@gmail.com

concerning the solidifying front-reinforcing particle interactions, which are based on thermodynamic and kinetic considerations. Zubko et al. [14] proposed the thermal conductivity criterion, according to which, engulfment will occur when the thermal conductivity of the liquid is higher than that of the reinforcing particles. This theory was refined by Surrapa and Rohatgi [15]. Many other theories have been based on the thermal conductivities and the thermal fields developed during the solidification of cast composites such as in the works of Rohatgi et al. [16], Hadji [17], Garvin and Udaykumar [18] whereas the importance of other factors such as interfacial characteristics and crystallographic compatibility are addressed in the works of Kaptay [19, 20], Ohta and Suito [21, 22] and Schaffer et al. [23]. An analytical model for the interaction between an insoluble particle and an advancing solid/liquid interface has been presented by Shangguan et al. [24]; in this model, they addressed the concept of the critical velocity of the interface, V_{cr}, below which the particle will be pushed and above which the particle will be engulfed. They also showed the dependence of V_{cr} on surface energy changes and particle size.

Many other models have been based on the concept of solidification front critical velocity [25–42] such as in the works of Stefanescu et al. [31], Han and Hunt [32], Juretzko et al. [33], Shibata et al. [34], Kimura et al. [35], Catalina et al. [36], Mukherjee and Stefanescu [37], Mukherjee et al. [38], Youssef et al. [39], Garvin et al. [40, 41] and Stefanescu [42]. Stefanescu and Dhindaw [43], summarized the parameters affecting the critical velocity for the different cases of solidification conditions (unidirectional–multidirectional) and the different morphologies of the solidification front (planar, cellular, dendritic). They concluded that V_{cr} can be described qualitatively as:

$$V_{cr} = f(\Delta\sigma, 1/\eta, 1/r, K_1/K_p, G),$$

where $\Delta\sigma$ is the change in the interfacial energies, η is the viscosity of the melt, r is the particle radius, K_1 and K_p are the thermal conductivities of the liquid and the particle, respectively, and G the temperature gradient ahead of the solidification front. For summarized approaches on the phenomena concerning the interaction of insoluble particles with the solidification front in cast metal matrix composites, the reader is strongly recommended to refer to the review works of Asthana and Tewari [44] and Asthana [45].

Although a variety of Al-alloys have been investigated as potential matrix systems (Al, Al–Si, Al–Mg, Al–Mg–Si, Al–Cu, etc.), the research works have mainly been concentrated on SiC and Al_2O_3 particulate reinforcements [1–6, 46–54]. However, several experimental efforts have been focused on the utilization of TiC particles as potential reinforcements of Al alloys. For example, Contreras et al. [55] and Albiter et al. [56] produced Al–Mg/TiC and Al-2024/TiC composites, respectively, by melting infiltration techniques; Selcuk and Kennedy [57] prepared an Al/TiC master composite of high TiC content (over 50 vol.%) by reaction synthesis of elemental powders; Shyu and Ho [58], Premkumar and Chu [59], Kharti and Koczak [60] and Sahoo and Koczak [61] produced Al/TiC composites through the reaction of carbonaceous gas with Ti dissolved in an Al melt; Karantzalis et al. [13] produced Al/TiC composites by a stir casting process. Limited work on WC as potential reinforcing phase for aluminium alloys can be found; for example, the work of Karantzalis et al. [13] is reported.

In this investigation, TiC and WC particles were chosen as the reinforcing phase because of their properties and their metallic character [62, 63]. The latter is an important factor for sufficient wetting, when in contact with aluminium melts, without the necessity of interfacial chemical reactivity. Such behaviour can lead to great affinity for molten aluminium, reduced tendency for particle agglomeration, good particle distribution in the melt and development of strong interfaces. Especially in the case of TiC, its good wetting behaviour towards Al melts have been shown in the works of Frumin et al. [64, 65], Contreras et al. [66] and Lopez and Kennedy [67].

In this work, the selection of the matrix material was based on its potential applications and solidification features. During the last decades, cast aluminium alloys have extensively been used by the automotive industry for the production of engine components as potential replacements of cast iron [68].

It is on this basis, where the scope of the present work stands: to investigate the potential to produce aluminium matrix composites by the facilitation of halide salts, as well as the solidification behaviour of a novel matrix–particulate combination.

Experimental procedure

The technique adopted for the production of the examined MMCs, was a modified stir casting process based on the utilization of KBF_4 as a fluxing salt for the oxide phase removal from the surface of the Al melts. The overall process comprises the following steps: (a) mixing of reinforcement and salt equal quantities, (b) spreading of the mixture at the top of the molten alloy resting in a graphite crucible at 800 °C, (c) reaction between the salt and Al to form a slag that dissolves the surface oxide, (d) insertion of the reinforcing particles into the melt, (e) removal of the slag, (f) slight and gentle mechanical stirring of the slurry and (g) pouring into a cylindrical type steel mould of 1.5 cm inner diameter and 15 cm height.

The matrices employed were: Al 6060 (0.35–0.6 Mg, 0.30–0.6 Si, 0.10–0.30 Fe), Al 356 (6.5–7.5 Si, 0.20–0.45 Mg, Fe the main impurity), Al 319 (5.5–6.5 Si, 3.0–4.0 Cu, Zn the main impurity), Al 2007 (3.3–4.6 Cu, 0.40–1.8 Mg, 0.8–1.5 Pb, Zn, Fe and Si the main impurities), Al–7Mg–5Si, Al–20Cu and Al–20Cu with Ni and Fe additions (<2 wt% for both of them). All compositions are reported in wt%. The reinforcement volume fraction was 3–5 vol.%, unless otherwise stated. The size of the TiC particles was −325 mesh (less than 44 μm), whereas the size of the WC particles was smaller than 10 μm.

Specimens where cut, mounted and prepared for inspection. Standard metallographic procedures were applied (grinding by 80, 200, 500, 800 and 1000 SiC grit papers followed by polishing by 6, 3 and 1 μm diamond suspensions). Metallographic inspection was conducted by the use of a LEICA 4000 optical microscope. Particle content measurements were conducted by the aid of the 'Image J' image analysis software. The technique is based on the calculation of the different area portions of the involved phases, which are coloured differently, through the use of the appropriate optical microscope images. XRD analysis was carried out using the Bruker D8 Advance X-ray diffractometer with a Cu–Kα lamp. SEM inspection was carried out using the JEOL 5600 system equipped with an Oxford Instruments EDS analysis system.

Results and discussion

Particle incorporation

The uniform dispersion of the ceramic particles in the molten matrix is a crucial factor for the resulting microstructure and is directly linked with the wetting characteristics of the involved phases. Good wetting is primarily responsible for the introduction of the ceramic phase into the molten alloy. TiC and WC are compounds of strong metallic nature owing to the presence of Ti and W. Such a metallic character is reported to improve the wetting behaviour of TiC and WC when in contact with metallic melts [62, 63]. The Al–TiC and Al–WC wetting behaviour is somehow more complicated. In general, the system is characterized by good wettability, low contact angles and good interfacial bonding [69]. However, such behaviour is achieved only when the surface oxide layer covering the Al melt is removed or dissociated. This removal or dissociation occurs only at high temperatures (>900 °C) [69]. At such high temperatures, the system becomes intensively reactive; the dissociation of TiC and WC and the formation of Al_4C_3 and/or Al_3Ti, Al_3W compounds take place at or close to the interfacial area [62, 63, 69]. In general, such reactivity can improve wettability [62, 63]; however, the formation of new phases can alter dramatically the nature and the response of the reinforcement–matrix interface.

Another possible remedy for the oxide phase present on the melt surface is its dissolution. The beneficial action of Na- and K-based fluoride and chloride salts to dissolve the oxide phases present on the surface of the melt has been documented in several experimental efforts [70, 71]. The use of such fluxes in the production of composites ensures minimization of the oxide phases [12, 13] and consequent improvement of the wetting behaviour. Such a good wetting led to the successful incorporation of the TiC and WC particles into the different Al alloy matrices tested. This good wetting is also responsible for the satisfyingly uniform particle distributions. As being described in the following paragraphs, the clusters observed could be either inherited from the precursor master powder material or a result of the solidifying front–particle interactions.

During conventional manufacturing of cast metal matrix composites, extensive mechanical stirring is used in order to provide the necessary shear forces for both reinforcing phase insertion and precursor material cluster dissociation. In the present study, such an intensive mechanical stirring was not adopted because the main target of the effort was to evaluate the ability of the salts to incorporate the ceramic phase into the melt without any other supportive mechanism being present.

Microstructures

Figure 1a–f presents the microstructures of the Al 6060, Al 356, Al 319, Al–7Mg–5Si, Al–20Cu and Al–20Cu (containing Fe and Ni additions) composites reinforced with TiC ceramic particles. The distribution of the reinforcing particles is satisfyingly uniform consisting of both isolated and clustered particles. In the case of the Al 6060, Al 319 and Al–7Mg–5Si composites, both isolated and clustered particles are mainly located at the grain boundaries. In the case of the Al 356 and Al–20Cu composites, the particle clusters are located at the grain boundaries, whereas the isolated particles are found both at the grain boundaries and within the grains. The existence and/or presence of particle clusters could be associated, in general, with three possible reasons: (a) unbroken particle clusters inherited from the precursor powder material that did not dissociate during the insertion into the melt, (b) particle clustering prior to solidification, due to poor wettability between the liquid metal and the ceramic reinforcement and (c) particle clustering owing to particle pushing by the solidification front during the solidification stage. Amongst these possible reasons, the second one is the most unlikely to take place, since the nature of the manufacturing process adopted in this effort ensures that the involved phases (liquid metal–ceramic reinforcement) express their real

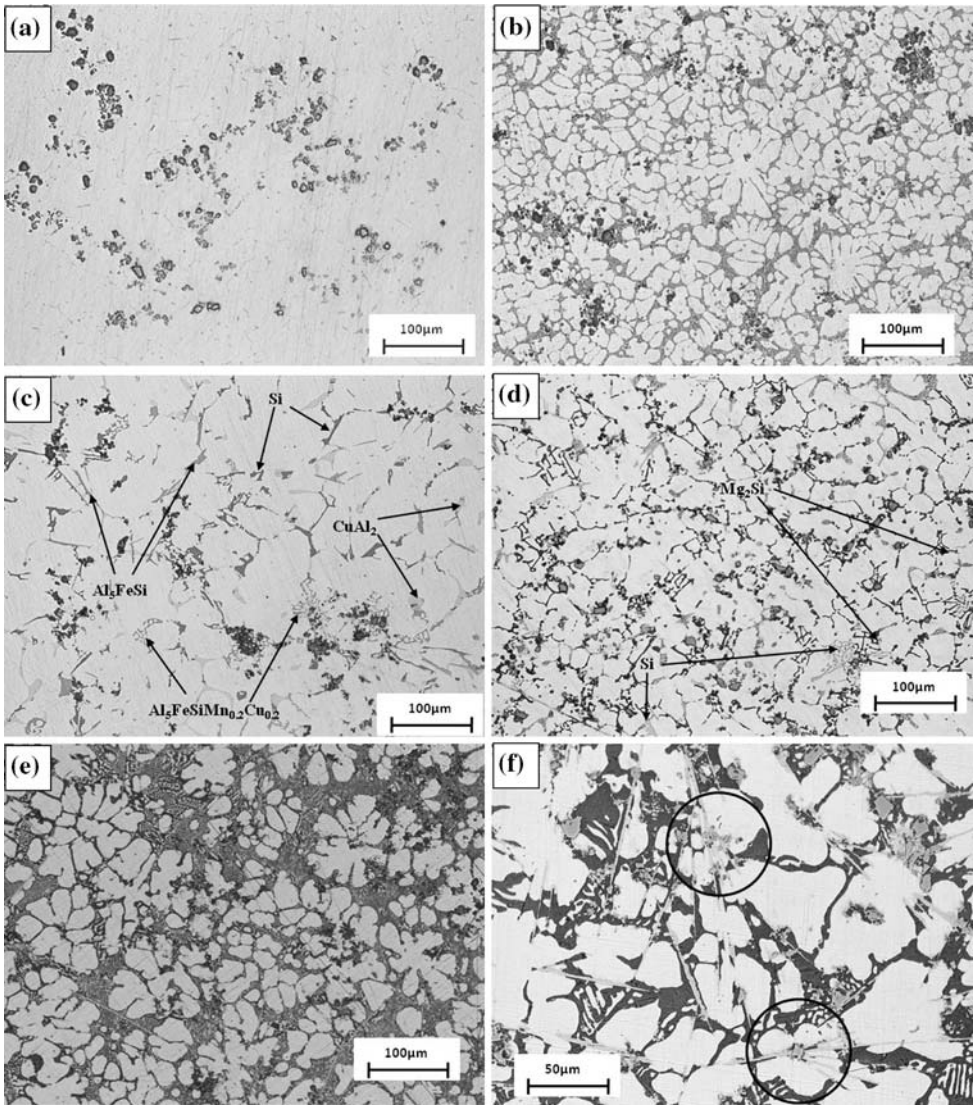

Fig. 1 **a** Isolated and clustered TiC particles evenly distributed in an Al 6060 matrix. **b** Microstructure of Al 356–TiC composite. Particles are located both at the grain boundaries (isolated and clustered) and within the grains (isolated). **c** Microstructure of Al 319–TiC composite. Particles are located at the gain boundaries and they are associated with the presence of various intermetallic phases. **d** Microstructure of Al–7Mg–5Si–TiC composite. Particles are located at the areas of the lastly solidified liquid and they are associated with the Mg_2Si intermetallic phase. **e** Microstructure of Al–20Cu–TiC composite. Particles are located both at the areas of the lastly solidified liquid (isolated and clustered) and within the grains (isolated). **f** Microstructure of Al–20Cu–TiC composite with additions of Fe and Ni. Particles are located both at the areas of the lastly solidified liquid and within the grains and they are related with the formation of needle-like intermetallic phases

wetting characteristics which, as fore-mentioned, are very good.

Another important issue to be mentioned is that in most of the cases, the presence of the particles (either isolated or clustered) at the grain boundaries and the areas of the lastly solidified liquid, is associated with the formation and growth of various intermetallic and eutectic phases. For the Al 319 composite (Fig. 1c), for instance, the TiC particles are associated with intermetallic phases such as Si, Al_5FeSi, $CuAl_2$ and $Al_5FeSiMn_{0.2}Cu_{0.2}$ and in the case of Al–7Mg–5Si (Fig. 1d) with Mg_2Si. Similar behaviour is observed in the case of the Al–20Cu composite with Ni and Fe additions (Fig. 1f), where the TiC particles are related with the formation of complex Al–Cu–Fe–Ni intermetallic substances. This particle-intermetallic phase interrelation is expected, since both TiC and alloying additions are segregated at the areas of the lastly solidified liquid during the solidification stage.

Figure 2 presents the microstructure of an Al–TiC composite with a high volume fraction of reinforcement (25–30 vol.%) composite. It is quite obvious that through the modified casting technique used to produce the composites, it is possible to accomplish the insertion of a relatively high amount of ceramic phase into the molten alloy; this indicates that the method has a significant versatility regarding the amount of the reinforcing phase additions.

Figure 3 shows the microstructure of Al 6060 (Fig. 3a) and Al 2007 (Fig. 3b) reinforced with WC particles. The particle concentration for the first composite is relatively high ($\sim$10 vol.%) and the particle distribution is characterized by the presence of extended clusters. These clusters have most likely been inherited from the raw powder material and did not dissociate during their incorporation into the melt. Both the non-intensive mechanical stirring during processing and the small WC particle size (<10 μm

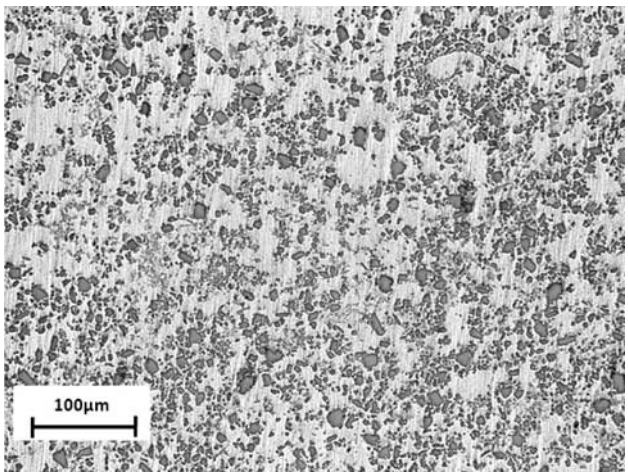

Fig. 2 Microstructure of an Al 6060–TiC composite with a high volume fraction of reinforcement (25–30 vol.%)

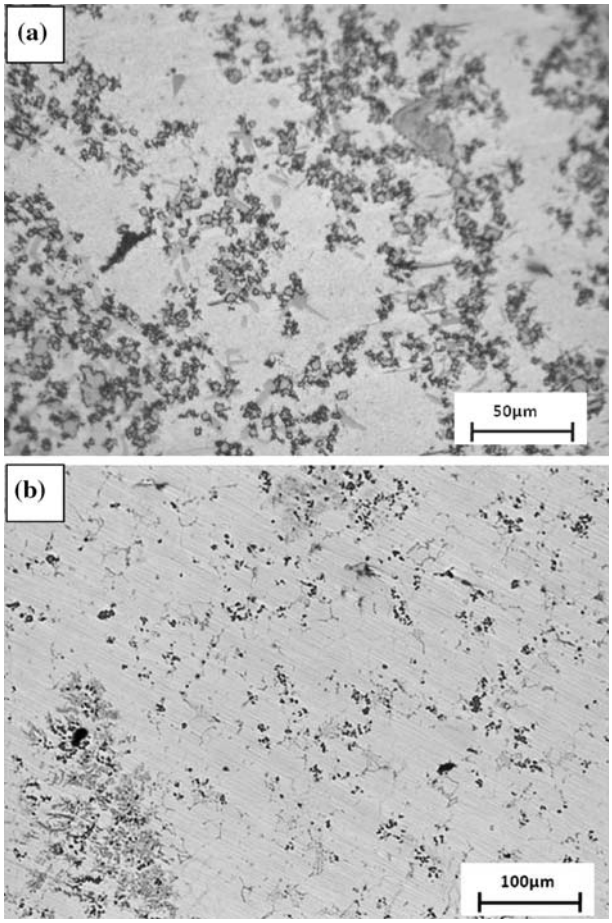

Fig. 3 **a** Microstructure of Al 6060–WC composite showing particle clustering. Reaction products in the vicinity of the reinforced phase can also be observed. **b** Microstructure of Al 2007–WC composite showing extensive particle clustering

compared to −325 mesh for the TiC particles) can account for this lack of dissociation. The distribution of WC particles in the Al 2007 matrix (Fig. 3b) is more uniform with both isolated and non-extensive particle clusters being evenly dispersed.

Interfacial reactivity

Figure 4a and b presents the particle–matrix interfacial area after SEM examination, for two different composite materials with the same alloy matrix (Al 6060) but with TiC and WC as the reinforcing phase, respectively. The micrograph of the TiC reinforced composite (Fig. 4a) shows the formation of Al boride phases which are the results of the reaction of KBF_4 (salt used as a fluxing agent during the production step) with molten Al. Similar reaction products have been reported by other researchers [72–74]. It is also important to note, that at the periphery of the TiC particles there is no

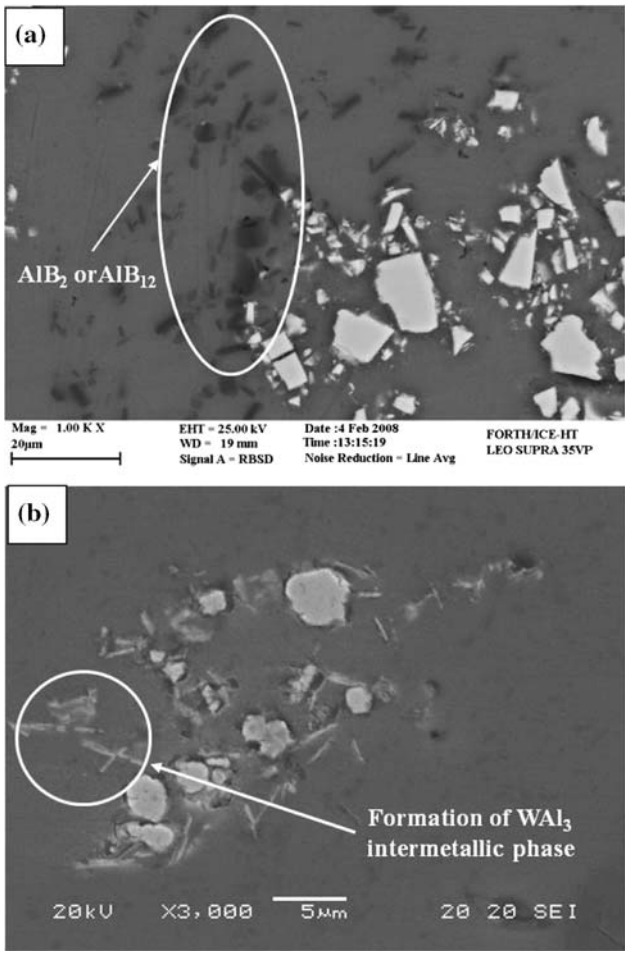

Fig. 4 **a** SEM micrograph of Al 6060–TiC composite. No significant evidence of reaction products at the matrix–particle interface can be recognized. The formation of boride phases can be observed as a result of chemical reaction between molten Al and KBF_4 (the latter having been used as a fluxing/wetting agent). **b** SEM micrograph showing the presence of WAl_3 intermetallic phase as a result of reaction between molten Al and WC particles

strong evidence of any disintegration and consequent formation of extensive reaction products, such as Al_4C_3 and Al_3Ti, as reported in other works [75]. This lack of reactivity (at least for this depth of examination) can be attributed to the short production period (3–5 min) that cannot provide enough time for severe reactivity. On the contrary, as shown in Fig. 4b, in the case of the WC reinforcing phase, extensive reaction products have been formed in the vicinity of the particles; EDX analysis of these products revealed the formation of WAl_3 phase. Based on this observation, it is postulated that WC has reacted with Al leading to the formation not only of aluminide but also Al_4C_3, which, however, at this depth of examination is difficult to be recognized. This WC reactivity compared to that of TiC, can be explained by the fact that for the temperature and time of processing, WC is more thermodynamically unstable [63].

Particle–solidification front interactions

Figure 1 shows that the grain morphology of primary α-Al is dendritic for all the different matrix types. In some instances, this dendritic morphology is more profound and intensive (i.e. Al 356, Al-20%Cu) and in other instances is less profound (i.e. Al 319, Al 2007, Al 6060). Irrespectively of the grain morphology, it was observed that particle clusters are located at the grain boundaries and the areas of the lastly solidified liquid, whereas isolated particles can be located both at the grain boundaries and within the grains; the latter case was observed especially for alloys with heavily dendritic structure, such as Al 356 and Al-20%Cu.

This particle behaviour, regarding the solidification front of dendritic morphology, can be predicted by the

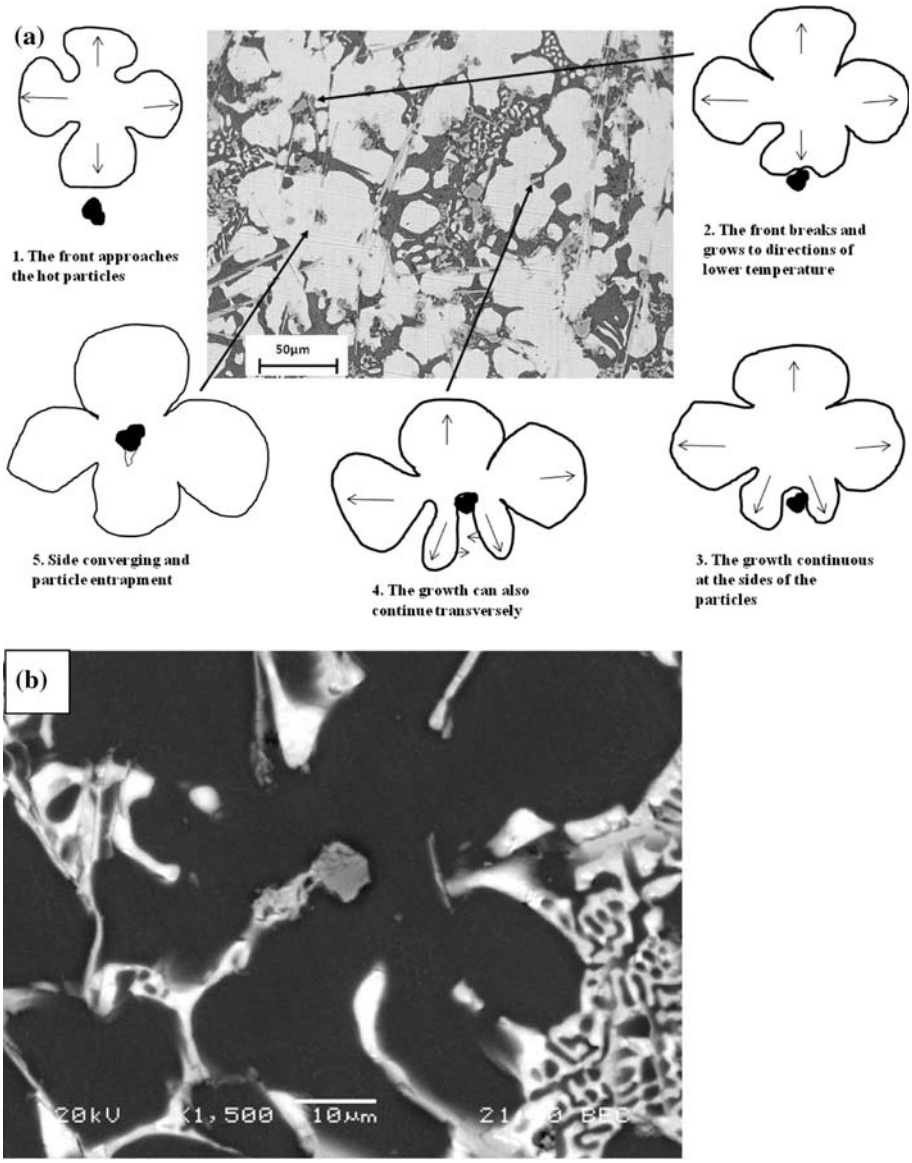

Fig. 5 **a** The possible mechanism explaining the entrapment of reinforcement particles by the primary-α grains. **b** SEM micrograph showing particle entrapment in the primary α-grain, one step before the final entrapment

work of Stefanescu and Dhindaw [43] by means that, for the examined cast composite, the corresponding critical velocity is higher than the actual solidification front velocities. This, in turn, led to both isolated and clustered particles at the grain boundaries and the areas of the lastly solidified liquid.

In the case of heavily dendritic morphologies it was also observed that particles had been entrapped within the grains. This observation is also compatible with the speculations of Stefanescu and Dhindaw [43], according to which such an entrapment is possible under certain circumstances: the large particles/clusters (relatively to the actual dendrite size) are pushed by the dendrite tips, whereas the small particles can be entrapped in the grains. The difference of the thermal conductivities between particles and molten alloy, can explain such an entrapment.

Figure 5a summarizes the proposed mechanism of particle entrapment (in the case of the Al–20Cu matrix reinforced with TiC particles) in few steps: (a) A growing dendrite approaches the TiC particle. (b) The TiC particle has a lower heat extraction rate than that of the melt, owing to its poor thermal conductivity (~20 W/m K) as compared to that of the molten alloy (~95 W/m K). This means that the particle remains hotter for prolonged time and keeps the surrounding liquid at higher temperature than the rest of the melt. (c) The growing dendrite tip realizes the existence of a hot liquid front that retards its further growth. (d) For the dendrite growth to continue, the tip splits into two side-branches aside the particle towards directions of lower temperature. (e) The growth of the split branches continues until they reach such a distance that the liquid is no longer affected by the presence of the hot particle. In this case, the branches can start growing towards the direction which is normal to their initial growing direction. As the two branches coincide, the particle is entrapped within the solidified grain. Figure 5b shows particle entrapment within the solidified primary α-grains just before the final entrapment. Another important observation arising from the previously described mechanism is that the solidified grains have equiaxed morphology. This is due to the fact that the growing grain is evenly surrounded by hot particles, which means that there is no area free of particles that could provide a preferential dendrite growth direction.

The considerations stated in the previous paragraphs, in general explain the reinforcing particle behaviour during solidification. However, a rather peculiar situation, as far as the particle location is concerned, is shown in Fig. 6. Figure 6 shows the microstructure of an Al–20Cu/TiC composite that has been cast into a preheated steel mould (~400 °C). This preheated mould results in slower solidification, i.e. lower solidification front velocity. Since in the case of casting into a mould at ambient temperature, the actual solidification front velocity was less than the critical one and no particle engulfment was observed, no particle engulfment would be expected, as well, in the case of preheated mould. However, Fig. 6 reveals the existence of particles within the primary α-Al grains that seem engulfed rather than entrapped. However, it is observed that these particles have very small size. If there was any possibility of particle engulfment under these unfavourable conditions, this should be for the large particles and not for the small ones, as the qualitative approach of Stefanescu and Dhindaw [43] describes. A possible explanation for such behaviour could be as follows: Under these solidification conditions where the solidification front velocity is slow, the time for the solidification front to reach the small particles is increased. At the same time, these small particles, despite their poor thermal conductivity, possess a lower thermal content than that of the large particles, due to their size. Hence, by the time the solidification front reaches them, they have enough time to follow the heat

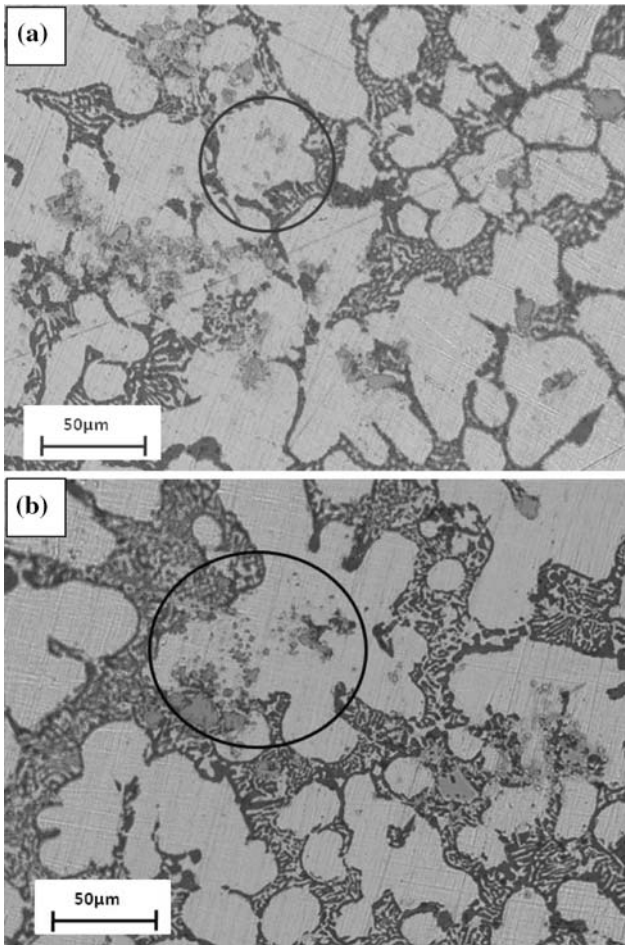

Fig. 6 **a**, **b** Microstructure of Al–Cu–TiC composite cast in preheated mould, showing the engulfment of small particles by the primary-α grains

extraction and lose their thermal content, thus reducing their temperature. Therefore, when the solidification front is close to them, they are not that hot and can be engulfed. It should be mentioned that such an approach may indicate that the critical velocity concept and the parameters affecting it, such as the thermal conductivities and the particle size, should be reconsidered in order to take into account, amongst others, the actual thermal content of the particles.

Conclusions

1. TiC and WC particles were successfully introduced into various Al alloy melts (Al 6060, Al 356, Al 2007, Al 319, Al–7Mg–5Si, Al–20Cu, Al–20Cu–Fe–Ni) to produce 3–5 vol.% (or higher volume fraction) composite materials through the use of a modified cast-based process.
2. The production technique uses KBF_4 as a fluxing agent that melts on the surface of the molten alloy and forms a slag that dissolves the surface oxide film. This dissolution allows the ceramic particles and the molten alloy to express their real wetting characteristics, making the particle insertion very favourable.
3. Particle distribution can be characterized as uniform consisting of both isolated and clustered particles. Isolated particles are located both within the grains and at the grain boundaries. Particle clusters are located at the grain boundaries and the areas of the lastly solidified liquid. In cases of high alloying additions, particle clusters are associated with the formation and growth of various intermetallic and other eutectic phases.
4. No signs of intensive reactivity between TiC and molten Al are recognized. On the other hand, in the case of WC reinforcement, a WAl_3 intermetallic phase is observed indicating its degradation and reaction with Al.
5. Particle location was explained in terms of the solidification front critical velocity and the difference in thermal conductivity between the reinforcing particles and the melt. However, observations of small particle engulfment under low solidification rate, can be the motive for reconsidering some of the parameters affecting the solidification front critical velocity concept.

References

1. Lloyd DJ (1999) Int Mater Rev 39:1
2. Rohatgi PK, Asthana R, Das S (1986) Int Mater Rev 31:115
3. Mortensen A, Jin I (1992) Int Mater Rev 37:101
4. Rohatgi PK, Ray S, Asthana R, Narendranath CS (1993) Mater Sci Eng A162:163
5. Asthana R, Tewari SN (1993) Compos Manuf 4(1):3
6. Howe JM (1993) Int Mater Rev 38(5):233
7. Nakae H, Fujii H, Shinohara T, Zhao BR (1993) In: Miravete A (ed) Proceedings of the ninth international conference on composite materials, pp 255–262
8. Wu Y, Zhang J, Lavernia EJ (1994) Mater Trans 25B:135
9. Kaptay G (1996) Mater Sci Forum 215–216:459
10. Kaptay G (2001) In: Pandey AB, Kendig KL, Watson TJ (eds) Affordable metal–matrix composites for high performance applications. TMS, ISBN: 0-87339-500-X, pp 71–99
11. Kaptay G (2005) J Mater Sci 40:2125. doi:10.1007/s10853-005-1902-2
12. Kennedy AR, Karantzalis AE (1999) Mater Sci Eng A264(1–2):122
13. Karantzalis AE, Wyatt S, Kennedy AR (1997) Mater Sci Eng A237(2):200
14. Zubko AM, Lobanov VG, Nikonova VV (1973) Sov Phys Crystallogr 18(2):239
15. Surrapa MK, Rohatgi PK (1981) J Mater Sci 16(2):562. doi:10.1007/BF00738658
16. Rohatgi PK, Pasciak K, Narendranath CS (1994) J Mater Sci 29:5357. doi:10.1007/BF01171548
17. Hadji L (2001) Phys Rev E 64:051502-1-6
18. Garvin JW, Udaykumar HS (2004) J Cryst Growth 267:724
19. Kaptay G (2001) Metall Mater Trans A 32A:993
20. Kaptay G (2002) Mater Trans 33A:1869
21. Ohta H, Suito H (2006) ISIJ Int 46:22
22. Ohta H, Suito H (2006) ISIJ Int 46:472
23. Schaffer PL, Miller DN, Dahle AK (2007) Scripta Mater 57:1129
24. Shangguan D, Ahuja S, Stefanescu DM (1992) Metall Trans A 23:669
25. Ulmann DR, Chalmers B, Jackson KA (1964) J Appl Phys 35(10):2986
26. Cisse J, Bolling GF (1971) J Cryst Growth 10:67
27. Cisse J, Bolling GF (1971) J Cryst Growth 11:25
28. Bolling GF, Cisse J (1971) J Cryst Growth 10:55–66
29. Chernov AA, Temkin DE, Melnikova AM (1976) Sov Phys Crystallogr 21(4):369
30. Stefanescu DM, Dhindaw BK, Kacar SA, Moitra A (1988) Metall Trans A 19:2847
31. Stefanescu DM, Phalniker RV, Pang H, Ahuja S, Dhindaw BK (1995) ISIJ Int 35(6):700
32. Han Q, Hunt JD (1995) ISIJ Int 35(6):693
33. Juretzko FR, Dhindaw BK, Stefanescu DM, Sen S, Curreri PA (1998) Metall Mater Trans A 29A:1691
34. Shibata H, Yin H, Yoshinaga S, Emi T, Suzuki M (1998) ISIJ Int 38(2):149
35. Kimura S, Nabeshima Y, Nakajima K, Mizoguchi S (2000) Metall Mater Trans B 31B:1013
36. Catalina AV, Mukherjee S, Stefanescu DM (2000) Metall Mater Trans A 31A:2559
37. Mukherjee S, Stefanescu DM (2004) Metall Mater Trans 35A:613
38. Mukherjee S, Sharif MAR, Stefanescu DM (2004) Metall Mater Trans 35A:623
39. Youssef YM, Dashwood RJ, Lee PD (2005) Composites A 36:747
40. Garvin JW, Yang Y, Udaykumar HS (2007) Int J Heat Mass Transfer 50:2952
41. Garvin JW, Yang Y, Udaykumar HS (2007) Int J Heat Mass Transfer 50:2969
42. Stefanescu DM (2007) Trans Ind Inst Metals 60(2–3):79
43. Stefanescu DM, Dhindaw BK (1988) In: ASM metals handbook, vol 15 casting. ASM International, ISBN: 0-87170-021-2, pp 315–326
44. Asthana R, Tewari SN (1993) J Mater Sci 28:5414. doi:10.1007/BF00367810
45. Asthana R (1998) J Mater Sci 33:1679. doi:10.1023/A:1004308027679

46. Mussert KM, Vellinga WP, Bakker A, Van Der Zwaag S (2002) J Mater Sci 37:789. doi:10.1023/A:1013896032331
47. Hu C, Baker TN (1997) J Mater Sci 32:5047. doi:10.1023/A:1018653030270
48. Candan E, Atkinson HV, Jones H (2000) J Mater Sci 35:4955. doi:10.1023/A:1004838610567
49. Lopez VH, Kennedy AR (2005) J Mater Sci 40:2453. doi:10.1007/s10853-005-1974-z
50. Ureina A, Rodrigo P, Gil L, Escalera MD, Baldonero JL (2001) J Mater Sci 36:419. doi:10.1023/A:1004880629720
51. Hadianfard MJ, Ma Y-W (2000) J Mater Sci 35:1715. doi:10.1023/A:1004720300774
52. Khan TI, Miller S (2001) J Mater Sci 36:1307. doi:10.1023/A:1004870917957
53. Gomez De Salazar JM, Barrena MI (2002) J Mater Sci 37:1497. doi:10.1023/A:1014967324577
54. Zulfia A, Hand RJ (2002) J Mater Sci 37:955. doi:10.1023/A:1014395730170
55. Contreras A, Angeles-Chávez C, Flores O, Perez R (2007) Mater Character 58:685
56. Albiter A, Leon CA, Drew RAL, Bedolla E (2000) Mater Sci Eng A289:109
57. Selcuk C, Kennedy AR (2006) Mater Lett 60:3364
58. Shyu RF, Ho CT (2006) J Mater Process Technol 171:411
59. Premkumar MK, Chu MG (1995) Mater Sci Eng A202:172
60. Khatri S, Koczak M (1993) Mater Sci Eng A162:153
61. Sahoo P, Koczak M (1991) Mater Sci Eng A144:37
62. Eustathopoulos N, Nicolas MG, Drevet B (1999) In: Chan RW (ed) Wettability at high temperatures. Pergamon Materials Series, ISBN: 0-08-042146-6, p 300
63. Naidich JV (1981) Prog Surface Membr Sci 14:353
64. Frumin N, Frage N, Polak M, Dariel MP (1997) Scripta Mater 37:1263
65. Froumin N, Frage N, Polak M, Dariel MP (2000) Acta Mater 48:1435
66. Contreras A, Bedolla E, Perez R (2004) Acta Mater 52:985
67. Lopez VH, Kennedy AR (2006) J Colloid Interface Sci 298:356
68. Ovono D, Guillot I, Massinon D (2006) Scripta Mater 55:259
69. Rhee SK (1970) J Am Ceram Soc 53(7):386
70. Boghosian S, Goda A, Mediaas H, Ravlo W, Østvold T (1991) Acta Chem Scan Ser A45:145
71. Mediaas H, Vindstad JF, Østvold T (1997) Acta Chem Scan Ser A51:504
72. Fjellstedt J, Jarforfs AEW (2005) Mater Sci Eng A 413–414:527
73. Fjellstedt J, Jarforfs AEW, Svedsen L (1999) J Alloys Comp 283:192
74. Mahallaway NE, Taha MA, Jarfors AEW, Fredriksson H (1992) J Alloys Comp 292:221
75. Lopez VH, Scoles A, Kennedy AR (2003) Mater Sci Eng A356:316